

Table I. Representative K_1 Values from Ref 1

ref	A	solvent ^a	counterion	isotopic sub.	T (K)	K_1
1b	benzene	THF	K ⁺	D ₆ /H ₆	173	0.27
	benzene	THF	K ⁺	¹³ C ₆ / ¹² C ₆	173	0.48
1d	nitrobenzene	gas phase		¹⁵ N/ ¹⁴ N	305	1.02
	nitrobenzene	NH ₃	K ⁺	¹⁵ N/ ¹⁴ N	208	2.1
	nitrobenzene	NH ₃	Na ⁺	¹⁵ N/ ¹⁴ N	208	0.4
1e	benzophenone	HMPA	Na ⁺	carbonyl ¹³ C/ ¹² C	298	0.58
	fluorenone	HMPA	Na ⁺	carbonyl ¹³ C/ ¹² C	298	2.74

^aTHF = tetrahydrofuran, HMPA = hexamethylphosphoramide.

Table II. Cut-Off Model^a Calculations for K_1

A	isotope	T (K)	I	II	III	I'	II'	III'
nitrobenzene (Nbz)	¹⁵ N/ ¹⁴ N	208	0.98	1.02	1.57	1.09	1.13	1.70
		305	0.99	1.01	1.35	1.06	1.09	1.42
fluorenone (Flu)	carbonyl ¹³ C/ ¹² C	298	1.00	1.02				1.62

^aNeutral molecule A is unsolvated. I, II, and III refer to different anion models: I (I'), II (II'), and III (III') correspond to A⁻ (unsolvated), (A⁻)Y (singly solvated), and (A⁻)Y₅ (5-solvated), respectively. Geometry of A⁻ moiety is same as A. Y is atom with atomic mass 23.0 amu, but results depend only weakly on this mass. In (A⁻)Y, the Y atom is symmetrically bonded to both oxygens (Nbz) or to one oxygen (Flu). In (A⁻)Y₅, the four additional Y's are bonded in square-planar geometry to N (Nbz) or to carbonyl C (Flu). Force constants (fc's) in harmonic valence force field: I, II, III, and III'—Y—O, Y—N (Nbz), and Y—C (Flu) stretching fc's equal 20 md/Å, bending fc's involving Y were given values 2–5 md/Å; I, II, and III—all single (multiple) bond stretching fc's in A⁻ moiety 1.3 (0.7) of corresponding value in A; I', II', and III'—all stretching fc's involving N (Nbz) or carbonyl C (Flu) in A⁻ moiety twice the corresponding value in A.

A⁻ models. Important aspects of these models are described in the footnote. Relevant differences between valence force constants (fc's) in A and in the anionic species are given. Thus, II (II'), III (III') correspond to solvated (ion-paired) A⁻ with II (II') referring to (A⁻)Y and III (III') to (A⁻)Y₅. In III (III'), four Y atoms are bonded to the isotopically substituted atom with four Y—N (or Y—C) stretching fc's of very large magnitude (20 md/Å). This magnitude was chosen to calculate upper limits to ie's. In I, II, and III, single-bond stretching fc's in the A⁻ moiety were increased with respect to fc's in the A species, while multiple bond stretching fc's were decreased, as suggested by Khatkale and Devlin⁶ (actual magnitudes of increases and decreases here are somewhat arbitrary). By contrast in I', II', III', the stretching fc's in the A⁻ moiety which determine the ie were increased to twice their respective values in the A species, a choice again made to obtain upper limits to ie's. As expected, ie's are larger for III (III') than for I (I'). K_1 's for III' are quite high upper limits.

We compare the K_1 values for nitrobenzene ¹⁵N/¹⁴N in ref 1d with our results in Table II. The reported gas-phase result at 305 K lies within the range one might have expected from calculations I and I'. However, the value 2.1 reported at 208 K in NH₃ with potassium the counterion far exceeds the value obtained in calculation III', which is a high upper limit. One can equally well focus on the reported K_1 value 0.4 at 208 K when the counterion is sodium. This low value requires the fc's at the nitrogen atom in the A species to be very high compared to those in A⁻; without giving details, it is clear that the required fc changes are "unnatural". Considerations on vapor pressure ie's⁷ show that anomalously larger effects in the condensed phase nitrobenzene systems cannot be rationalized as an involvement of low-frequency motions of the condensed phase.

A few calculations are presented in Table II on fluorenone, which would equally well apply to benzophenone since the models

(6) Khatkale, M. S.; Devlin, J. P. *J. Chem. Phys.* **1979**, *70*, 1851; *J. Phys. Chem.* **1979**, *83*, 1636.

(7) Jancso, G.; Van Hook, W. A. *Chem. Rev.* **1974**, *74*, 689 and references therein.

for the two systems are similar. Clearly the large ¹³C/¹²C ie's reported in ref 1e for these systems are also problematic. No comment is made here on the D/H effects in ref 1 or on the ¹³C/¹²C effect in benzene; the reported magnitudes of these probably do not exceed easily set theoretical upper limits.

Thus, the large magnitudes of heavy atom isotope effects reported in ref 1 for K_1 require unreasonably large changes of force constants between A and A⁻; the results cannot be accepted as equilibrium ie's.

Registry No. ¹³C, 14762-74-4; ¹⁵N, 14390-96-6.

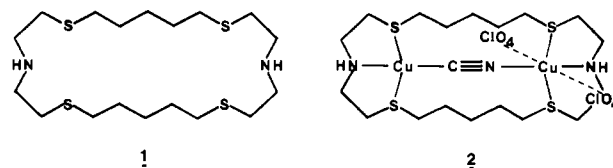
Mixed-Valence Cu(I)Cu(II) Macrocyclic Complex: A Result of a Cu(II)-Promoted Oxidation of Aziridines into Cyanide

Y. Agnus,* J. P. Gisselbrecht, R. Louis, and B. Metz

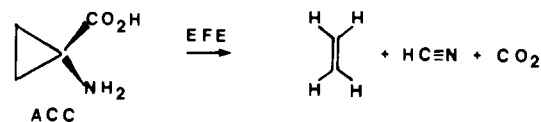
Institut de Chimie, Université
Louis Pasteur,[†] 1 rue Blaise Pascal
BP 296 R8, 67008 Strasbourg Cedex, France

Received July 20, 1988

During our investigation on activating properties of the binuclear [2CuC1]⁴⁺ system, we have studied its interaction with aziridine compounds. The *N*-methylaziridine in the presence of [2CuC1]⁴⁺ leads to cyanide ions producing a new binuclear mixed-valence copper(I,II) complex, **2**. The two metallic centers, bridged by



a cyanide ion, are enclosed in **1**.¹ The X-ray structure and physico-chemical properties of **2** provide a good opportunity to emphasize the expected cyanide binding mode in the mixed-valence derivative of hemocyanin^{2,3} depicted for the half-met CN form.⁴ It is also a new example of concerted interactions between binuclear complexes, substrates, and solvents in reactions involving multielectronic processes,⁵ and could be relevant to the role of the ethylene-forming enzyme (EFE) in the conversion of 1-aminocyclopropane carboxylic acid (ACC).^{6,7}



[†]UA405 CNRS: Electrochimie et Physico-chimie des complexes et des systèmes interfaciaux; IBMC CNRS: Laboratoire de Cristallographie Biologique.

(1) (a) Agnus, Y. L. In *Copper Coordination Chemistry: Biochemical and Inorganic Perspectives*; Karlin, K. D., Zubieta, J. A., Eds.; Adenine Press: New York, 1983; pp 371-393. (b) Agnus, Y.; Louis, R.; Gisselbrecht, J. P.; Weiss, R. *J. Am. Chem. Soc.* **1984**, *106*, 93-102.

(2) (a) Gaykema, W. P. J.; Hol, W. G. J.; Vereijken, J. M.; Soeter, N. M.; Bak, H. J.; Beintema, J. J. *Nature* **1984**, *309*, 23-29. (b) Linzen, B.; Soeter, N. M.; Riggs, A. F.; Schneider, H. J.; Schartau, W.; Moore, M. D.; Yokota, E.; Behrens, P. Q.; Nakashima, H.; Takagi, T.; Nemoto, T.; Vereijken, J. M.; Bak, H. J.; Beintema, J. J.; Volbeda, A.; Gaykema, W. P. J.; Hol, W. G. J. *Science* **1985**, *229*, 519-524. (c) Gaykema, W. P. J.; Volbeda, A.; Hol, W. G. J. *J. Mol. Biol.* **1985**, *187*, 255-275.

(3) Solomon, E. I.; Penfield, K. W.; Wilcox, D. E. *Struct. Bonding* **1983**, *53*, 1-57.

(4) (a) Himmelwright, R. S.; Eickman, N. C.; Solomon, E. I. *J. Am. Chem. Soc.* **1979**, *101*, 1576-1586. (b) Himmelwright, R. S.; Eickman, N. C.; LuBien, C. D.; Solomon, E. I. *J. Am. Chem. Soc.* **1980**, *102*, 5378-5388.

(5) (a) Zanello, P.; Tamburini, S.; Vigato, P. A.; Mazzocchin, G. A. *Coord. Chem. Rev.* **1987**, *77*, 165-273. (b) Karlin, K. D.; Gultneh, Y. *Prog. Inorg. Chem.* **1987**, *35*, 219-327.

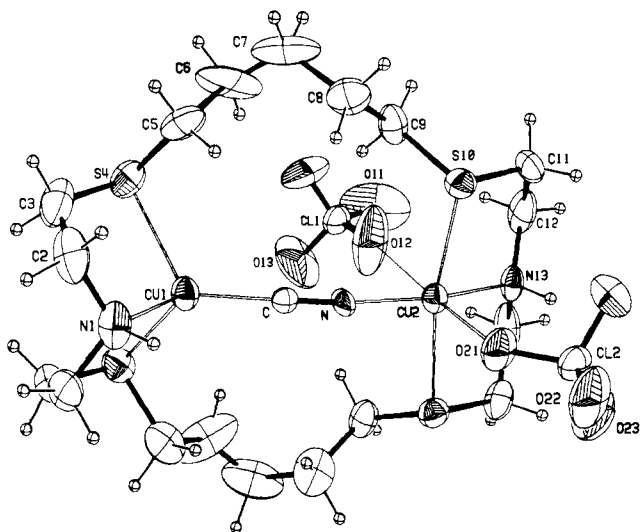
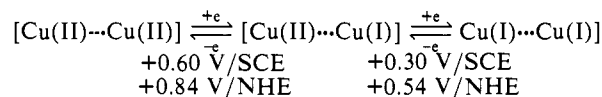


Figure 1. Perspective view of **2**. The complex lies on a mirror plane which contains the two nitrogens of **1**, the copper and cyanide ions, and the chlorine with two oxygen atoms of each perchlorate ion. Selected distances (Å) and angles (deg) are as follows: Cu1...Cu2 4.894 (4), Cu1-N1 2.11 (2), Cu1-S4 2.360 (5), Cu1-C 1.91 (2), Cu2-N13 1.99 (2), Cu2-S10 2.348 (4), Cu2-N 1.90 (2), Cu2-O21 2.44 (2), and Cu2-O12 3.14 (3); N1-Cu1-C 126.5 (7), N1-Cu1-S4 87.7 (3), C-Cu1-S4 120.8 (3), S4-Cu1-S22 105.1 (3), N13-Cu2-N 163.1 (7), N13-Cu2-S10 86.3 (1), N13-Cu2-O21 99.0 (6), N13-Cu2-O12 77.6 (6), N-Cu2-S10 94.9 (1), N-Cu2-O21 98.0 (7), S10-Cu2-S16 168.2 (2), S10-Cu2-O21 86.0 (1), and O21-Cu2-O12 176.5 (5).

Complex **2** is obtained by mixing copper(II) perchlorate, **1** and *N*-methylaziridine in a 2:1:1 ratio in aqueous ethanol-nitromethane solutions (see alternative procedures in ref 8). **2** crystallizes as brown tapered needles. Microanalysis,⁹ IR spectra, and X-ray structure determination are evidence of the cyanide ion in **2** (although absent in any starting material). **2** exhibits a strong C≡N IR stretching frequency at 2120 cm⁻¹. Its electronic spectrum in CH₃CN presents a broad band at 600 nm ($\epsilon = 790 \text{ mol}^{-1} \text{ L cm}^{-1}$; ligand field and $\pi S \rightarrow \text{Cu}^{\text{II}}\text{LMCT}$) and an intense absorption at 390 nm ($\epsilon = 7100 \text{ mol}^{-1} \text{ L cm}^{-1}$; $\sigma S \rightarrow \text{Cu}^{\text{II}}\text{LMCT}$). Magnetic susceptibility measurements (1.6–300 K) show that **2** displays a constant magnetic moment of 1.75 μ_B per dinuclear unit, consistent with the mixed-valence formulation.^{10a} The solid-state X-band EPR spectra exhibit a symmetrical line with *g* values of 2.0543 at 300 K and 2.0602 at 140 K,^{10b} indicating no electron delocalization between the Cu(II) and Cu(I) centers.

The structure of **2** is shown in Figure 1.¹¹ The two copper centers are separated by 4.894 (4) Å and linked by an end-to-end bridging cyanide in a slightly bent fashion (Cu1-C-N = 176.6 (7)° and Cu2-N-C = 169.0 (8)°).^{12,13} The stereochemistry of Cu1 closely approximates a tetrahedron, while that of Cu2 is square bipyramidal showing clearly that Cu1 is the cuprous and Cu2 the cupric center.

The electrochemical study of **2** in nitromethane shows, by cyclic voltammetry, a one-electron oxidation and a one-electron reduction:



The two monoelectronic processes are quasireversible.¹⁴ The [2CuC1]⁴⁺ ions with the exogenous chloride or azide ligands act as dielectronic donor-acceptor systems,¹ whereas with cyanide the mixed-valence species is obtained. Examples containing exogenous ligands capable of influencing the whole properties are known; however, the mixed-valence compounds were only electrochemically or spectroscopically characterized.^{15–22} The stabilization of **2** in the solid state and in solution results from the widely separated redox potentials for the two monoelectronic steps, +0.84 and +0.54 V vs NHE. They are lying on each side of a critical potential delimiting cupric or cuprous state stabilizing, which explains the obtention of **2** from both the bis-copper(II) or the bis-copper(I) complex.⁸ Indeed it is interesting to point out that cupric complexes exhibiting redox potential greater than ca. +0.6 V vs NHE undergo spontaneous evolution into cuprous compounds through homogeneous redox processes which are solvent independent.^{17,24–26} Concomitant oxidation implying water, molecular oxygen, and hydroxide ions has been established in the case of nitriles,²⁷ and this hypothesis seems in agreement with the

(6) (a) Adams, D. O.; Yang, S. F. *Trends Biochem. Sci.* **1981**, *6*, 161–164. (b) Peiser, G. D.; Wang, T. T.; Hoffman, N. E.; Yang, S. F.; Liu, H. W.; Walsh, C. T. *Proc. Natl. Acad. Sci. U.S.A.* **1984**, *81*, 3059–3063.

(7) (a) Pirrung, M. C. *J. Am. Chem. Soc.* **1983**, *105*, 7207–7209. (b) Pirrung, M. C. *Biochemistry* **1986**, *25*, 114–119. (c) Pirrung, M. C.; McGeehan, G. M. *J. Org. Chem.* **1983**, *48*, 5144–5146. (d) Pirrung, M. C.; McGeehan, G. M. *J. Org. Chem.* **1986**, *51*, 2103–2106. (e) Baldwin, J. E.; Jackson, D. A.; Adlington, R. M.; Rawlings, B. J. *J. Chem. Soc., Chem. Commun.* **1985**, 206–207.

(8) (a) Stoichiometric amounts of **1** (in toluene-nitromethane solution), copper(II) nitrate (in aqueous ethanolic solution), and potassium cyanide are mixed together. A large excess of sodium perchlorate is added to the resulting solution. (b) The binuclear copper(I) complex [2Cu(CN)C1](ClO₄) obtained under inert atmosphere from [Cu(CH₃CN)₄](ClO₄), with **1** and potassium cyanide in acetonitrile, rapidly affords **2** when exposed to air.

(9) Anal. Calcd (Found) for C₁₉H₃₈Cl₂Cu₂N₃O₈S₄: C, 29.92 (30.01); H, 5.02 (5.16); N, 5.51 (5.49).

(10) (a) Magnetic susceptibility measurements were carried out with a Faraday-type magnetometer displaying magnetic fields till 0.7 T. The independence of the susceptibility against the magnetic field was checked at room temperature, 77 and 4.2 K. The magnetic data were corrected for diamagnetism estimated as $-368 \times 10^{-6} \text{ cm}^3 \text{ mol}^{-1}$. (b) The EPR experiments were performed with a Bruker ER 420X band spectrometer at Institut C. Sadron, CNRS, Strasbourg, France.

(11) Crystal data for **2**: fw = 762.77; orthorhombic, *Pnma*; *a* = 11.371 (1) Å, *b* = 12.961 (2) Å, *c* = 20.940 (2) Å; *V* = 3086.3 Å³; *D*_{calcd} = 1.642 g cm⁻³, *D*_{obsd} = 1.636 g cm⁻³; *Z* = 2; $\mu(\text{Cu K}\alpha)$ = 62.1 cm⁻¹. The best of the tested crystals has given a limited data set due to its small size and diffraction characteristics. 911 independent reflections with *I* ≥ 2 σ (*I*) (Enraf-Nonius CAD4), empirically corrected for absorption were used to solve the structure by direct methods, Fourier and least-squares techniques. The agreement factors $R = \sum(|F_o| - |F_c|) / \sum|F_o|$ and $R_w = [\sum w(|F_o| - |F_c|)^2 / \sum w|F_o|^2]^{1/2}$, where $w = [1/\sigma(F_o)]^2$, reached respectively 0.073 and 0.091.

(12) Dunaj-Jurco, M.; Ondrejovic, G.; Melnik, M.; Garaj, J. *Coord. Chem. Rev.* **1988**, *83*, 1–28.

(13) (a) Jungst, R.; Stucky, G. *Inorg. Chem.* **1974**, *13*, 2404–2408. (b) Duggan, D. M.; Hendrickson, D. N. *Inorg. Chem.* **1974**, *13*, 1911–1916. (c) Landee, C. P.; Wicholas, M.; Willett, R. D.; Wolford, T. *Inorg. Chem.* **1979**, *18*, 2317–2318.

(14) Cyclic voltammograms are included as Supplementary Material.

(15) Olmstead, M. M.; Musker, W. K.; Kessler, R. M. *Inorg. Chem.* **1981**, *20*, 151–157.

(16) Acholla, F. V.; Takusagawa, F.; Bowman Mertes, K. *J. Am. Chem. Soc.* **1985**, *107*, 6902–6908.

(17) Latour, J. M.; Limosin, D.; Rey, P. *J. Chem. Soc., Chem. Commun.* **1985**, 464–466.

(18) (a) Gagné, R. R.; Spiro, C. L.; Smith, T. J.; Hamann, C. A.; Thies, W. R.; Shiemke, A. K. *J. Am. Chem. Soc.* **1981**, *103*, 4073–4081. (b) Gagné, R. R.; Koval, C. A.; Smith, T. J.; Cimolino, M. C. *J. Am. Chem. Soc.* **1979**, *101*, 4571–4580.

(19) Long, R. C.; Hendrickson, D. N. *J. Am. Chem. Soc.* **1983**, *105*, 1513–1521.

(20) (a) Mandal, S. K.; Nag, K. *Inorg. Chem.* **1983**, *22*, 2567–2572. (b) Mandal, S. K.; Thompson, L. K.; Nag, K.; Charland, J. P.; Gabe, E. J. *Inorg. Chem.* **1987**, *26*, 1391–1395.

(21) Mazurek, W.; Bond, A. M.; Murray, K. S.; O'Connor, M. J.; Wedd, A. G. *Inorg. Chem.* **1985**, *24*, 2484–2490.

(22) Bianchi, A.; Mangani, S.; Micheloni, M.; Nanini, V.; Orioli, P.; Paoletti, P.; Seghi, B. *Inorg. Chem.* **1985**, *24*, 1182–1187.

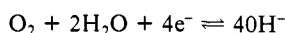
(23) Latimer, W. M. *The Oxidation States of the Elements and their Potentials in Aqueous Solutions*; 2nd ed.; Prentice-Hall: Englewood Cliffs, NJ, 1952.

(24) Gisselbrecht, J. P.; Gross, M. *Adv. Chem. Ser.* **1982**, *201*, 110–137.

(25) Tikkanen, W. R.; Kruger, C.; Bomben, K. D.; Jolly, W. L.; Kaska, W. C.; Ford, P. C. *Inorg. Chem.* **1984**, *23*, 3633–3638.

(26) Mandal, S. K.; Thompson, L. K.; Gabe, E. J.; Lee, F. L.; Charland, J. P. *Inorg. Chem.* **1987**, *26*, 2384–2389.

Latimer redox potential of +0.40 V vs NHE for the half reaction²³



The drastic anodic shift of a redox potential observed in **2** can be understood in view of the redox potential of the couple Cu(II)/[Cu^I(CN)₂]⁻ in basic medium which is as high as +1.103 V vs NHE.²³

The oxidation of *N*-methylaziridine into cyanide is unprecedented. It requires deprotonation steps, proved by the strong increase of the reaction rate in basic media. The ease of the reaction in nitromethane in respect of other solvents is likely due to the participation of the basic CH₂NO₂⁻ form. The analogy with the function of the EFE in the biological oxidation of ACC^{6,7} lies in the production of CN⁻, involving two sequential one-electron oxidation steps at positive potentials. The system [2CuC^I]⁴⁺ plays the role of oxidant, giving the [2CuC^I]²⁺ complex, while *N*-methylaziridine is oxidized in cyanide. [2CuC^I]²⁺, in the presence of the generated cyanide and under air, leads to the mixed valence compound **2**.⁸

Supplementary Material Available: Tables of atomic coordinates and thermal parameters and cyclic voltammograms with related peak parameters (3 pages); tables of observed and calculated structure factors (5 pages). Ordering information is given on any current masthead page.

(27) (a) Schibler, W.; Kaden, T. A. *J. Chem. Soc., Chem. Commun.* **1981**, 603-604. (b) Curtis, N. J.; Hagen, K. S.; Sargeson, A. M. *J. Chem. Soc., Chem. Commun.* **1984**, 1571-1573. (c) Drew, M. G. B.; Yates, P. C.; Trocha-Grimshaw, J.; McKillop, K. P.; Nelson, S. M. *J. Chem. Soc., Chem. Commun.* **1985**, 262-263.

Striking Changes Observed in Key Acyl-Enzyme Linkages by Resonance Raman Experiments Near 77 K

P. J. Tonge, H. Lee, L. R. Sans Cartier, B. P. Ruzsicska, and P. R. Carey*

*Division of Biological Sciences
NRC, Ottawa, Ontario, Canada K1A 0R6*

Received September 6, 1988

The thermal processes occurring in an enzyme's active site are of high interest in attempting to delineate the efficient action of an enzyme on its bound substrate.¹⁻³ Questions such as the local temperature, the means of energy migration, the interchange among conformational substates,⁴ and the thermalization of vibrational modes along the reaction pathway are often posed without the support of experimental data. Since resonance Raman (RR) spectroscopy provides a vibrational spectrum associated with enzyme-substrate linkages^{5,6} and since the vibrational spectrum is sensitive to conformation and dynamical fluctuations, comparison of normal- and low-temperature RR data on enzyme-substrate complexes provides access to some of the changes occurring in the active site upon thermalization.

We report here low-temperature RR data for two acyl-enzyme complexes involving papain,⁷ *N*-benzoylglycine dithioacyl- and

(1) Welch, G. R.; Somogyi, B.; Damjanovich, S. *Prog. Biophys. Mol. Biol.* **1982**, *39*, 109.

(2) Careri, G.; Fasella, P.; Gratton, E. *Ann. Rev. Biophys. Bioeng.* **1979**, *8*, 69.

(3) Cooper, A. *Prog. Biophys. Mol. Biol.* **1984**, *44*, 181.

(4) Frauenfelder, H.; Parak, F.; Young, R. D. *Ann. Rev. Biophys. Biophys. Chem.* **1988**, *17*, 451.

(5) Carey, P. R.; Storer, A. C. *Pure Appl. Chem.* **1985**, *57*, 225.

(6) Carey, P. R.; Storer, A. C. *Ann. Rev. Biophys. Bioeng.* **1984**, *13*, 25.

(7) Cryogenic RR studies have been used in an attempt to detect anhydride-like acyl-enzyme intermediates of carboxypeptidase-A (Hoffman, S. J.; Chu, S. S.-T.; Lee, H.; Kaiser, E. T.; Carey, P. R. *J. Am. Chem. Soc.* **1983**, *105*, 6971) and in several studies of photodissociation involving heme proteins (see: Sassaroli, M., et al. *J. Am. Chem. Soc.* **1988**, *27*, 2496). Here we are concerned with the temperature-dependent changes occurring within well-characterized dithioacyl papain intermediates which are indefinitely (but reversibly) stabilized by freezing the reaction mixture.

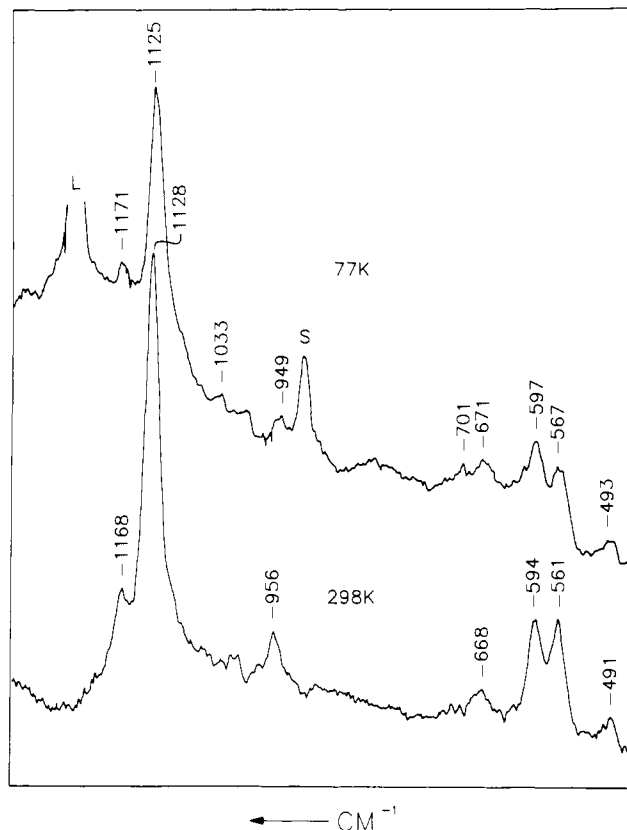


Figure 1. RR spectra of *N*-benzoylglycine dithioacyl papain in solution at room temperature (bottom); in ice matrix near 77 K (top). L = laser plasma line, S = peak due to CH₃CN used to carry substrate into solution.

methoxycarbonyl-L-phenylalanyl-glycine (PheGly) dithioacyl papain which are from a relatively "poor" and "good" substrate, respectively. For both intermediates, freezing in an ice matrix at 77 K results in a change in the C_α-CS(thiol) torsional angle in a direction away from that expected for the transition state for deacylation—i.e., a change consistent with deactivation. Moreover, at 77 K both intermediates show major RR intensity enhancement of a mode associated with the C-S linkage from cysteine-25⁶ in the enzyme's active site.

Upon freezing a reaction mixture containing *N*-benzoylglycine dithioacyl papain to ca. 250 K the intense 1128 cm⁻¹ RR peak (Figure 1) moves to 1125 cm⁻¹ (note that data at 250 K are *not* shown in Figure 1; we have RR spectra from 12 separate samples at 250 K; all show the small shift in the 1128 cm⁻¹ feature). This could be due to the phase change associated with freezing, which commonly brings about changes in vibrational frequencies. An alternative explanation is that the shift to 1125 cm⁻¹ is brought about by a 10–15° reduction in Ψ', the NHC-CS (thiol) torsional angle (see below). Upon reducing the temperature to 77 K an additional change occurs in the 668 cm⁻¹ feature in the form of major intensity enhancement (≈1.8-fold relative to other RR features), and a shoulder appears near 700 cm⁻¹ (Figure 1).⁹ Since the 668- and 700-cm⁻¹ bands are probably both due to ν_{S-C} (cysteine), the detection of the additional 700-cm⁻¹ feature is evidence for conformational heterogeneity in cysteine-25's S-C-C linkages.

(8) Brocklehurst, K.; Willenbrock, F.; Salih, E. Cysteine Proteinases. A chapter in *Hydrolytic Enzymes*; Neuberger, A., Brocklehurst, K., Eds.; Elsevier: Amsterdam, 1987.

(9) RR spectra are obtained by using 324 nm Kr⁺ excitation, a Spex triplemate and intensified diode array detection (Carey, P. R.; Sans Cartier, L. R. *J. Raman Spectrosc.* **1983**, *14*, 271). Low-temperature data were obtained by using back-scattering geometry from the sample in a helium cryostat modified so that the sample could rotate and move in the vertical plane (Sans Cartier, L. R.; Tonge, P. J.; Carey, P. R. *Ind. J. Phys.*, in press).